Subcellular Golgi localization of stathmin family proteins is promoted by a specific set of DHHC palmitoyl transferases

Aurore D. Levy[a], Véronique Devignot[a], Yuko Fukata[b,c], Masaki Fukata[b], André Sobel[a], and Stéphanie Chauvin[a]

[a]INSERM U 839, Université Pierre et Marie Curie, UMR-S839, and Institut du Fer à Moulin, F-75005, Paris, France; [b]Division of Membrane Physiology, Department of Cell Physiology, National Institute for Physiological Sciences, Aichi 444–8787, Japan; [c]PRESTO, Japan Science and Technology Agency, Tokyo 102–0075, Japan

ABSTRACT **Protein palmitoylation is a reversible lipid modification that plays critical roles in protein sorting and targeting to specific cellular compartments. The neuronal microtubule-regulatory phosphoproteins of the stathmin family (SCG10/stathmin 2, SCLIP/stathmin 3, and RB3/stathmin 4) are peripheral proteins that fulfill specific and complementary roles in the formation and maturation of the nervous system. All neuronal stathmins are localized at the Golgi complex and at vesicles along axons and dendrites. Their membrane anchoring results from palmitoylation of two close cysteine residues present within their homologous N-terminal targeting domains. By preventing palmitoylation with 2-bromopalmitate or disrupting the integrity of the Golgi with brefeldin A, we were able to show that palmitoylation of stathmins 2 and 3 likely occurs at the Golgi and is crucial for their specific subcellular localization and trafficking. In addition, this membrane binding is promoted by a specific set of palmitoyl transferases that localize with stathmins 2 and 3 at the Golgi, directly interact with them, and enhance their membrane association. The subcellular membrane–associated microtubule-regulatory activity of stathmins might then be fine-tuned by extracellular stimuli controlling their reversible palmitoylation, which can be viewed as a crucial regulatory process for specific and local functions of stathmins in neurons.**

Monitoring Editor
Erika L. F. Holzbaur
University of Pennsylvania

Received: Oct 15, 2010
Revised: Mar 10, 2011
Accepted: Mar 29, 2011

INTRODUCTION

Protein palmitoylation modulates diverse aspects of neuronal development and synaptic transmission (el-Husseini Ael and Bredt, 2002; Bijlmakers and Marsh, 2003; Resh, 2006). In particular, by regulating the appropriate localization of numerous proteins, palmitoylation is a crucial process that operates during all steps of neuronal differentiation and specification (Huang and El-Husseini, 2005; Resh, 2006; Linder and Deschenes, 2007; Fukata and Fukata, 2010). Among neuronal proteins the subcellular localizations of which are controlled by protein palmitoylation, stathmin-related proteins, namely stathmin 2/SCG10, stathmin 3/SCLIP, and stathmin 4/RB3 (Sobel, 1991; Ozon *et al.*, 1997, 1998; Curmi *et al.*, 1999; Mori and Morii, 2002; Lachkar *et al.*, 2010) are peripheral palmitoylated proteins (Di Paolo *et al.*, 1997; Charbaut *et al.*, 2005; Chauvin *et al.*, 2008) that play specific and complementary roles in the formation and maturation of the nervous system (Ozon *et al.*, 1998; Curmi *et al.*, 1999). Indeed, while stathmin 2 controls growth cone expansion (Morii *et al.*, 2006; Poulain and Sobel, 2007) and axonal elongation (Grenningloh *et al.*, 2004), stathmin 3 is involved in regulating axonal branching and dendritic formation and/or maturation (Poulain and Sobel, 2007; Poulain *et al.*, 2008). Similarly to the ubiquitous soluble member of these family proteins (stathmin 1), stathmin-related proteins are known to regulate microtubule dynamics (Belmont *et al.*, 1996; Curmi *et al.*, 1997; Jourdain *et al.*, 1997; Gigant *et al.*, 2000, 2005; Charbaut *et al.*, 2001; Ravelli *et al.*, 2004) by sequestering free tubulin with various efficacies (Charbaut *et al.*,

This article was published online ahead of print in MBoC in Press (http://www.molbiolcell.org/cgi/doi/10.1091/mbc.E10-10-0824) on April 6, 2011.

Address correspondence to: Stéphanie Chauvin (stephanie.chauvin@inserm.fr) or André Sobel (andre.sobel@inserm.fr).

Abbreviations used: 2-BP, 2-bromopalmitate; ABE, acyl-biotin exchange; BFA, brefeldin A; CM, chloroform–methanol; DIV, day in vitro; DTT, dithiothreitol; ER, endoplasmic reticulum; GFP, green fluorescent protein; HA, hemagglutinin peptide; HAM, hydroxylamine; Ig, immunoglobulin; LB, lysis buffer; NEM, *N*-ethylmaleimide; PAT, palmitoyl acyl transferase; PFA, paraformaldehyde; PSD-95, postsynaptic density protein of 95 kDa; SCG10, superior cervical ganglia-10; SCLIP, SCG10-like-protein; SLD, stathmin-like domain.

2001) through their C-terminal "stathmin-like domain" (SLD). Like for stathmin 1, the microtubule-destabilizing activity of stathmin 2 is regulated by multiple phosphorylation within its SLD (Gavet *et al.*, 1998; Charbaut *et al.*, 2001; Grenningloh *et al.*, 2004; Togano *et al.*, 2005). For instance, JNK1 phosphorylation regulates the activity of stathmin 2 on microtubule depolymerization and axonal development (Tararuk *et al.*, 2006; Poulain and Sobel, 2010).

The N-terminal palmitoylation of stathmin-related proteins promotes their specific anchoring to the cytosolic leaflet of Golgi membranes and their subsequent vesicular trafficking along dendrites and axons (Stein *et al.*, 1988; Di Paolo *et al.*, 1997; Lutjens *et al.*, 2000; Gavet *et al.*, 2002; Tararuk *et al.*, 2006; Poulain and Sobel, 2010). This specific subcellular localization results from the cooperation of two separate targeting signals present within their common N-terminal A domain (Charbaut *et al.*, 2005). Indeed, cooperation of a membrane-anchoring subdomain (m) carrying a palmitoylation motif with two close cysteine residues (Cys22 and Cys24 for stathmin 2; see Figure 1A) (Di Paolo *et al.*, 1997; Charbaut *et al.*, 2005) and a Golgi-specifying motif (subdomain n: AYKEKMKEL) drives unrelated fused proteins specifically to Golgi/vesicles (Charbaut *et al.*, 2005). This specific localization was completely abolished when the two sites of palmitoylation were mutated into alanine within the full-length stathmin 2 (C22A/C24A) (Di Paolo *et al.*, 1997), suggesting that cysteine palmitoylation is a crucial feature for specific subcellular localization of stathmins.

Palmitoylation, through a thioester linkage of a 16-carbon saturated fatty acid to a cysteine residue, is a reversible posttranslational modification. It is characterized by a relatively rapid turnover, allowing proteins to shuttle between the cytoplasm and intracellular organelles (Rocks *et al.*, 2006; Chisari *et al.*, 2007). Similarly to phosphorylation, palmitoylation is dynamically regulated by specific cellular stimuli (Wedegaertner and Bourne, 1994; El-Husseini Ael *et al.*, 2002; Tsutsumi *et al.*, 2008). Depalmitoylation of postsynaptic density protein of 95 kDa (PSD-95) is regulated by neuronal activity and promotes the removal of PSD-95 from synapses (el-Husseini Ael and Bredt, 2002), which in turn controls synaptic strength (El-Husseini Ael *et al.*, 2002) and illustrates the pivotal role of palmitoylation in regulating protein trafficking and function. The dynamic regulation of palmitate cycling is fine-tuned by palmitoyl acyl transferases (PATs) and palmitoyl protein thioesterases (Smotrys and Linder, 2004; Resh, 2006). PATs emerged from their identification in yeast as transmembrane proteins containing a DHHC (Asp-His-His-Cys) motif followed by a cysteine-rich domain (Bartels *et al.*, 1999; Lobo *et al.*, 2002; Roth *et al.*, 2002; Linder and Deschenes, 2004). At least 23 mammalian DHHC proteins exist, and systematic screening with more than 20 palmitoylated proteins has identified specific enzyme–substrate pairs (Iwanaga *et al.*, 2009; Fukata and Fukata, 2010). Besides their catalytic DHHC domain, individual DHHC proteins have some regulatory regions that would recruit specific substrates or regulators (Huang *et al.*, 2009).

Differential palmitate cycling on stathmin-related proteins could provide a potential mechanism for controlling their neuronal activity in addition to their SLD phosphorylation. To shed light on the pathway of stathmin-related protein palmitoylation, we have undertaken a detailed analysis of the DHHC proteins that palmitoylate stathmins 2 and 3, identifying a subset of Golgi enzymes that fulfill this function. We show that stathmin 2 and 3 palmitoylation is essential for their subcellular trafficking, hence pointing out regulation of stathmin subcellular localization, through regulation of their palmitoylation, as a crucial process to regulate their neuronal functions.

FIGURE 1: Stathmin 2 palmitoylation requires functional Golgi membranes. (A) Preceding their C-terminal SLD (box, not to scale), the N-terminal targeting A domain of stathmins 2 and 3 (A2 and A3, respectively) can be divided into three subdomains (n, m, and c) based on their sequence conservation. Cysteines 22 and 24 (boxed) are two conserved residues that are known to be palmitoylated. Conserved hydrophobic and charged residues are highlighted in light or dark gray, respectively. (B) The level of stathmin 2 palmitoylation in 6 DIV cortical neurons in culture, treated or not (Control) with 2-BP or BFA was evaluated using the ABE assay (see *Materials and Methods*). T: total NEM quenched cell extract (1:20 volume); as a control, HAM cleavage of palmitates was omitted in the Tris reaction buffer. Stathmin 2 was revealed on Western blots with specific antibodies. Biotinylated, originally palmitoylated stathmin 2 appeared as a doublet (HAM, ABE line). The ABE signal was reduced by approximately one half of the control when cortical neurons were treated with either 2-BP or BFA. Results are representative of two separate experiments that gave similar results.

RESULTS

Palmitoylation of the N-terminal targeting domain of stathmin related-proteins being instrumental for their specific subcellular localization in neurons, we investigated the underlying molecular determinants and mechanisms as well as the enzymes responsible for this essential lipid modification.

Specific localization and trafficking of stathmins 2 and 3 result from palmitoylation at the Golgi

Targeting of stathmins 2–4 to the Golgi, vesicles, and growth cones requires palmitoylation of two cysteine residues (Cys22 and Cys24 for stathmins 2 and 3, Figure 1A) within their conserved N-terminal extensions (A domain) (Di Paolo *et al.*, 1997; Charbaut *et al.*, 2005; Chauvin *et al.*, 2008). To investigate whether the palmitoylation of stathmins 2 and 3 directly influence their trafficking, or whether this effect could be operating via other mechanisms, we took a double pharmacological approach. First, we prevented protein palmitoylation by treating neurons with 2-bromopalmitate (2-BP), an unmetabolized palmitate analog, and followed palmitoylation of stathmins 2–3 in vivo using the acyl-biotin exchange (ABE) assay (Roth *et al.*, 2006; Kang *et al.*, 2008) (Figure 1B and Supplemental Figure S1). This approach involves blockade of free thiols with *N*-ethylmaleimide (NEM), cleavage of the Cys-palmitoyl thioester linkage with hydroxylamine (HAM), and labeling of newly exposed thiols with a sulfhydryl-specific biotin labeling compound [biotin-HPDP; *N*-[6-(biotinamido)hexyl]-3′-(2′-pyridyldithio)propionamide]. The biotinylated proteins, reflecting their original palmitoylation, are subsequently pulled down with NeutrAvidin beads. A fraction of the total neuronal extract (T) and the NeutrAvidin pulled-down proteins (HAM/ABE) were analyzed by Western blot (Figure 1B and Supplemental Figure S1). As a control for the ABE assay, cortical neuron extracts were treated with Tris alone instead of HAM, which did not release free cysteines from palmitoylated proteins to be labeled by biotin and hence to be isolated by NeutrAvidin pull-down

(Tris/ABE). In contrast, a neuronal extract treated with HAM in the ABE assay identifies palmitoylated stathmin 2 (Figure 1B, Control) or stathmin 3 (Supplemental Figure S1, Control), as revealed with their corresponding antibodies (see *Materials and Methods*). Furthermore, this assay also revealed several biotinylated electrophoretic bands in cortical neurons that likely correspond to forms of stathmins 2 and 3 diversely palmitoylated within their membrane targeting A domain. When protein palmitoylation was prevented by treating cortical neurons with 2-BP for 24 h, palmitoylation levels of stathmins 2 and 3 were decreased by approximately one half (Figure 1B and Supplemental Figure S1). Furthermore, as a large proportion of stathmins 2 and 3 are localized at the Golgi complex, we examined the effect of Golgi disruption by brefeldin A (BFA) on stathmin palmitoylation (Figure 1B and Supplemental Figure S1). Indeed, by inactivating the ADP-ribosylation factor 1 (Klausner *et al.*, 1992), BFA blocks the export of membranes and proteins from the endoplasmic reticulum (ER) and results in a reversible functional and structural disruption of the Golgi complex (Fujiwara *et al.*, 1988; Lippincott-Schwartz *et al.*, 1989). As shown in Figure 1B and Supplemental Figure S1, BFA treatment of cortical neurons also inhibited the palmitoylation levels of stathmins 2 and 3 by approximately one half, suggesting that palmitoylation of stathmins 2 and 3 requires functional Golgi membranes either to deliver the proteins to a specific location or to facilitate the reaction itself. Therefore, Golgi targeting might be required for palmitoylation, and palmitoylation might be necessary for stabilization of stathmins 2 and 3 on Golgi membranes.

Because both 2-BP and BFA inhibit palmitoylation of stathmins, we examined their effects on subcellular localization of endogenous stathmins 2 and 3 in hippocampal neurons (Figure 2 and Supplemental Figure S2). As shown previously (Di Paolo *et al.*, 1997; Gavet *et al.*, 2002; Poulain and Sobel, 2007), endogenous stathmin 2 is present both at the Golgi, as evidenced by a colabeling with a Golgi marker (CTR433), and also along neurites in association with vesicle-like structures. Treatment with 2-BP (24 h, 100 μM) or BFA (4 h, 5 μg/ml) dramatically disrupted the Golgi localization of stathmins 2 and 3, with no major structural effect on the Golgi in the case of 2-BP (Figure 2A and Supplemental Figure S2A), but with a complete delocalization of CTR433 labeling to the ER after BFA treatment (colocalization with KDEL, an ER marker) (unpublished data). Furthermore, the vesicle-like localization of stathmins 2 and 3 was perturbed (Figure 2 and Supplemental Figure S2). Indeed, in addition to partial solubilization of stathmins 2 and 3, inhibition of palmitoylation after 2-BP or BFA treatment also led to the appearance of small punctae, differing from the usual vesicle labeling and depending on the drug treatments. These results suggest that these treatments not only prevented stathmin palmitoylation but also perturbed trafficking pathways from the Golgi complex. Nevertheless, these stathmin 2– or 3–labeled punctuate structures did not colocalize with the ER marker KDEL but partially overlapped the perinuclear pattern of redistributed CTR433 (Figure 2 and Supplemental Figure S2). Note that after both treatments an unexpected labeling was observed within the nucleus with stathmin 2 antibodies.

To quantify the partial solubilization observed by immunofluorescence, another set of treated neurons was used to perform cell fractionation experiments that separate neuronal extracts into soluble versus membrane fractions (Figure 2, C and D; Supplemental Figure S2, C and D). Whereas the major part of stathmins 2 and 3 were in the membrane fraction (approximately 70% and 60% of total stathmins 2 and 3, respectively) in untreated cells (control), prevention of protein palmitoylation with 2-BP or BFA (via Golgi disruption) treatment showed a significant enrichment of stathmins 2 and 3 in the cytosol (approximately 60% soluble vs. 40% still membrane bound). Note that both treatments resulted in a decrease of the total amount of stathmins 2 and 3.

Altogether, our data show that palmitoylation of stathmins 2 and 3 might occur at the Golgi complex and that this palmitoylation is responsible for their specific Golgi/vesicles localization. Our results therefore demonstrate that specific Golgi localization of stathmins 2 and 3 requires ongoing palmitoylation, and palmitoylation might be required for retention on Golgi membranes and for maintaining stathmin 2 and 3 trafficking.

A subset of potential specific PATs colocalizes with stathmins 2 and 3 at the Golgi in hippocampal neurons

Systematic characterization of subcellular localization of tagged DHHC proteins transfected in HEK293T cells showed that, among the 23 DHHC proteins cloned, most of them are localized in the ER and/or Golgi compartments (Ohno *et al.*, 2006). Because subcellular localization of DHHC PATs would provide a mechanism for regulating the subcellular localization of stathmin-related proteins, we performed immunofluorescence microscopy on cultured hippocampal neurons at 6 d in vitro (DIV) to follow and compare the subcellular localization of stathmins 2 and 3 with a set of nine DHHC PATs that were previously described as neuronal Golgi resident PATs.

First, we performed colabeling of endogenous stathmin 2 and DHHC2 or DHHC3, which are the only DHHC PATs for which specific antibodies were available. As shown in Figure 3A, endogenous DHHC2 is not accumulated at the Golgi complex but is distributed within neurites and the cell body as small vesicle-like structures, as already described by Noritake and colleagues (Noritake *et al.*, 2009). Higher magnification images of either the cell body or one neurite did not show overlapping labelings between DHHC2 and stathmin 2–positive vesicles. Conversely, endogenous DHHC3 specifically localized at the Golgi complex, as previously described (Keller *et al.*, 2004; Noritake *et al.*, 2009) and showed an extensive colocalization with stathmin 2 at this subcellular compartment (Figure 3A).

Due to the lack of appropriate antibodies for the other DHHC PATs described as Golgi-resident in HEK293T cells, their potential colocalization with stathmins in hippocampal neurons in culture could be assessed only by overexpression of tagged exogenous PATs. To validate this overexpression approach, we first compared the subcellular localization of endogenous versus exogenous DHHC2 and -3 as compared to that of endogenous stathmin 2 in transfected hippocampal neurons (Figure 3B). Similarly to what we observed with the endogenous DHHC2 labeling, overexpression of hemagglutinin peptide (HA)-tagged DHHC2 in neurons also displayed DHHC2 at vesicle-like structures within the soma and neurites, with a partial overlapping of DHHC2 and stathmin 2 labelings in the area of the Golgi complex as well as within neurites (Figure 3B). Furthermore, as already observed with the labeling of the endogenous protein (Figure 3A), overexpressed HA-tagged DHHC3 specifically localized to the somatic Golgi apparatus, as shown by a perfect colocalization with the CTR433 Golgi marker (Supplemental Figure S3), and displayed a high degree of colocalization with stathmins 2 and 3 at this subcellular localization (Figure 3B and Supplemental Figure S3A). Altogether, these data indicate that, in contrast to DHHC2, DHHC3 is a strictly Golgi-restricted DHHC PAT that perfectly colocalized with stathmins 2 and 3 at the Golgi, and suggest DHHC3 as a potent candidate to palmitoylate stathmins 2 and 3 at the Golgi complex. In addition, they clearly validate the tagged-DHHC protein overexpression approach to study their subcellular colocalization with endogenous stathmins in neurons in culture.

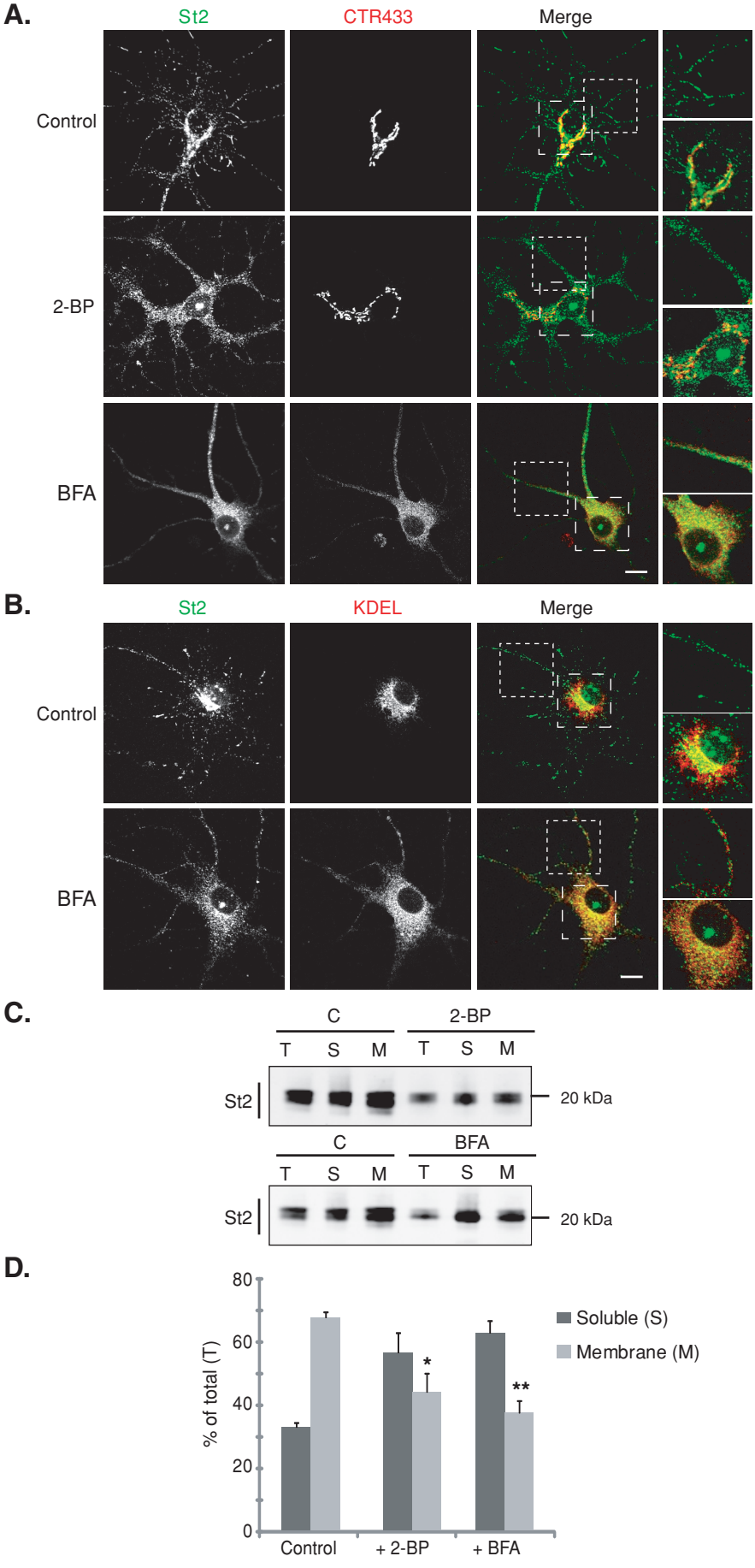

We therefore assessed the subcellular distribution of the other subset of DHHC PATs previously described to be Golgi-localized in HEK293T cells, by overexpressing their tagged-forms in hippocampal neurons in culture. Only DHHC7 and -17 were specifically restricted to the somatic Golgi as shown by their strict colocalization with the CTR433 marker (Figure 4A and Supplemental Figure S3A). Besides, higher magnification of merged images revealed a high degree of colocalization of these DHHCs with endogenous stathmins 2 (Figure 4A) and 3 (Supplemental Figure S3A) at the Golgi, whereas punctuate labeling within neurites only revealed endogenous stathmin 2 or 3. Conversely, overexpression of tagged DHHC9, -12, -15, or -22 in neurons not only showed these PATs at the Golgi, as evidenced by a colabeling with CTR433 (Supplemental Figure S4A), but also

FIGURE 2: Preventing palmitoylation leads to the dispersion of the Golgi pool of stathmin 2. Hippocampal neurons at 6 DIV were stained for stathmin 2 (St2, green) and for either the Golgi (CTR433, red) or the ER (KDEL, red). For each double labeling, a single-layer confocal image is shown. (A) In untreated neurons (control), stathmin 2 immunolabeling is present at the Golgi (colocalization with CTR433) and along neurites as vesicle-like structures. Treatments with 2-BP and BFA resulted in the dispersion of the Golgi pool of stathmin 2, whereas the vesicle-like localization was partially abolished. Higher magnification of the boxed neurite and soma regions in merged images better illustrates the dispersion of the Golgi stathmin 2 labeling as well as the small size of the remaining vesicle-like structures present after both treatments. (B) Following BFA treatment, stathmin 2 was not relocalized to the ER, neither in the soma nor within neurites (see higher magnification of the merged images). Bars = 10 µm. (C) The subcellular localization of stathmin 2 was analyzed after cell fractionation that separates the soluble (S) and membrane (M) fractions from total extracts (T) of untreated (C), 2-BP, or BFA-treated hippocampal neurons. Equivalent volumes of each fraction were analyzed by SDS–PAGE and Western blotted for stathmin 2. (D) Quantification of the membrane and soluble pools of stathmin 2 expressed as a percentile of stathmin 2 in the total extract. Whereas stathmin 2 was present in the majority of the membrane fraction in the control, it was significantly redistributed from the membrane to the soluble fraction after 2-BP or BFA treatment. Values are mean ± SEM (n = 3). The statistical significance of differences between stathmin 2 in membrane fractions when treated or not by 2-BP or BFA was assessed by a Student's *t* test. *$p < 0.05$, **$p < 0.01$.

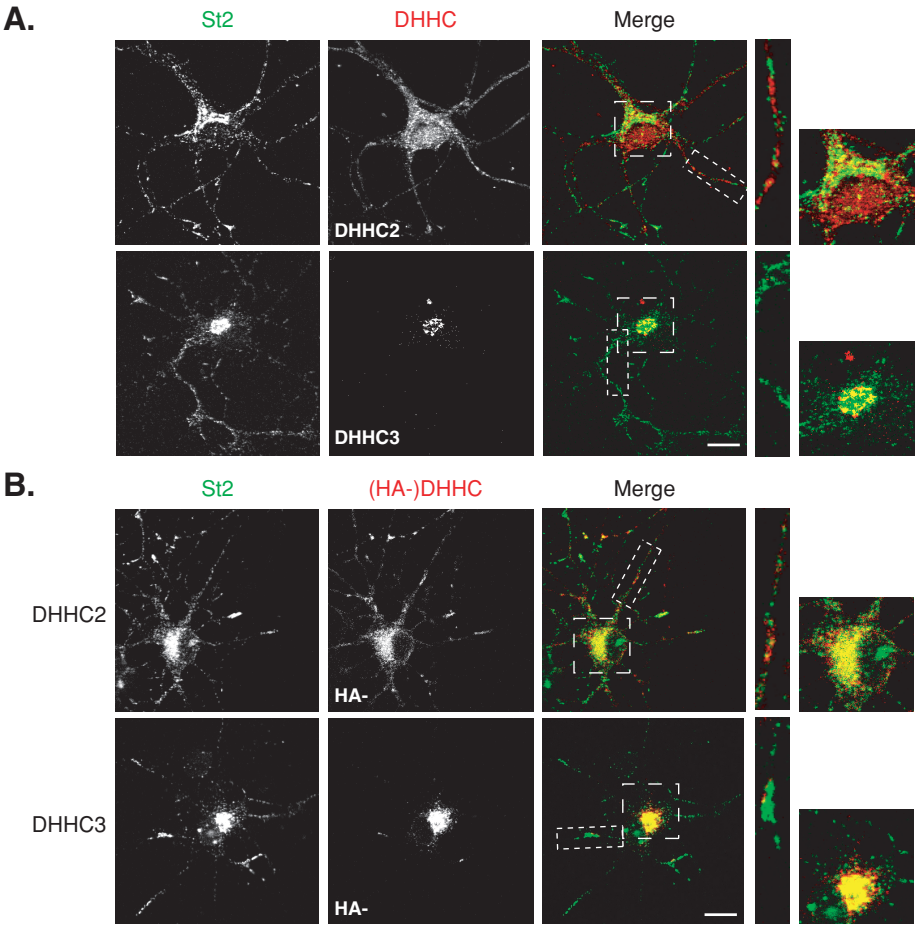

FIGURE 3: Relative subcellular distribution of stathmin 2 and endogenous DHHC2 and -3 in neurons. (A) Hippocampal neurons at 6 DIV were colabeled for stathmin 2 (St2, green) and DHHC2 or -3 (red). DHHC2 displayed a vesicle-like staining in the cell body and along neurites partially overlapping but not significantly colocalized with the Golgi and vesicle-like labeling of stathmin 2. The endogenous DHHC3 staining was concentrated at the Golgi where it displayed a significant colocalization with stathmin 2 labeling. (B) Hippocampal neurons transfected at 6 DIV with HA-DHHC2 or -3 were colabeled for endogenous stathmin 2 (St2, green) and for exogenous DHHCs (red) with anti-HA antibodies. Contrary to DHHC2, DHHC3 is a Golgi-restricted DHHC PAT that colocalized with stathmin 2 at the Golgi. DHHC2 staining showed a punctuate labeling within the soma and neurites that colocalized partially with the ones of stathmin 2. Bars = 10 μM; boxed areas in the merged images are shown at higher magnification.

revealed them to be associated with trafficking vesicles in the soma and processes (Figure 4B and Supplemental Figure S3B). Magnification of merged images showed that stathmins 2 and 3 partially colocalized with DHHC9, -12, -15, and -22 at the Golgi but did not follow the same trafficking along neurites because they did not display any colabeling in the processes. DHHC9 and -22 also localized within the ER as assessed by their extensive colocalization with the KDEL marker (Supplemental Figure S4B). Finally, DHHC4 did not display a clear Golgi localization (Figure 4B), but rather an extensive ER distribution within neurons (Supplemental Figure S4B). The other "Golgi localized" neuronal PATs DHHC8, -18, or -21, could not be visualized because of their weak overexpression in neurons.

Altogether, we showed that, among the nine "Golgi localized" DHHC PATs in HEK293 cells, only DHHC3, -7, and -17 are restricted to the Golgi in neurons, whereas DHHC12 and -15 are also distributed elsewhere in the soma and within neurites. Other DHHC PATs are either localized both at the Golgi and at the ER or are completely excluded from the Golgi. The strong colocalization observed between stathmin 2 or 3 and DHHC3, -7, -15, and -17 suggests that this last set of PATs might be good candidates to palmitoylate stathmins 2 and 3 at the Golgi in neurons.

The Golgi-localized DHHC3, -7, and -15 are specific PATs for stathmins 2 and 3

To determine whether DHHC PATs that are present at the Golgi can form stable complexes with the targeting domain of stathmins 2 (A2) and 3 (A3) in mammalian cells, myc-tagged DHHCs (-3, -7, -12, -15, -17, -18, or -22; Figure 5A and Supplemental Figure S5A) or HA-tagged DHHC3 (Figure 5B and Supplemental Figure S5B) were cotransfected into HeLa cells with the green fluorescent protein (GFP)-tagged domain A of stathmin 2 or 3 (A2 or A3). Solubilized extracts were immunoprecipitated with antibodies directed against the myc- or HA- tag of transfected DHHCs, and immunoprecipitates were examined by Western blot for the presence of GFP-tagged stathmin A domains. Immunoprecipitation of myc-DHHCs or HA-DHHC3 was confirmed by immunoblot using anti-myc or anti-HA antibodies, respectively. We could not succeed in performing efficient immunoprecipitation with DHHC21 (as already observed by Tsutsumi *et al.*, 2009) and -8 because of their weak expression. Coimmunoprecipitation of A2-GFP or A3-GFP with DHHC3, -7, -15, and -17 was readily detected with an antibody against the GFP epitope, confirming that these DHHCs can form stable complexes with A2 or A3 in transfected HeLa cells. No immunoreactive A2 or A3 was significantly observed after immunoprecipitation of the other Golgi-localized PATs, -12, -18, and -22 (Figure 5A and Supplemental Figure S5A). Interestingly, converse immunoprecipitation of A2- or A3-GFP using a GFP antibody only revealed an association with DHHC3, suggesting a better interaction of stathmins 2 and 3 with this specific PAT (Figure 5B and Supplemental Figure S5B). More precisely, DHHC3 seems to preferentially interact with one of the various forms of the targeting domains A2 or A3, appearing as a fast migrating band on Western blots (Figure 5B and Supplemental Figure S5B, arrowhead). Altogether, our results show that stathmins 2 and 3, through their specific A domain, can interact preferentially with DHHC3 but also with DHHC7, -15, and -17.

In parallel with these interaction experiments, we also examined the potential activities of all 23 DHHC PATs on palmitoylation of stathmins 2–4. We individually cotransfected the HA-tagged DHHC proteins with myc-tagged stathmin 2 into HEK293 cells and assessed palmitoylation of stathmin 2 by metabolic labeling with [^{3}H] palmitate. Among the 23 different DHHCs tested, only DHHC2, -3, -7, -15, and -21 significantly increased palmitoylation of stathmin 2 (Figure 6A). The highest activity was observed for DHHC3 and its closest homolog DHHC7. A somewhat lower stathmin 2 palmitoylation activity was also seen with the distant DHHC3 paralogs DHHC2,

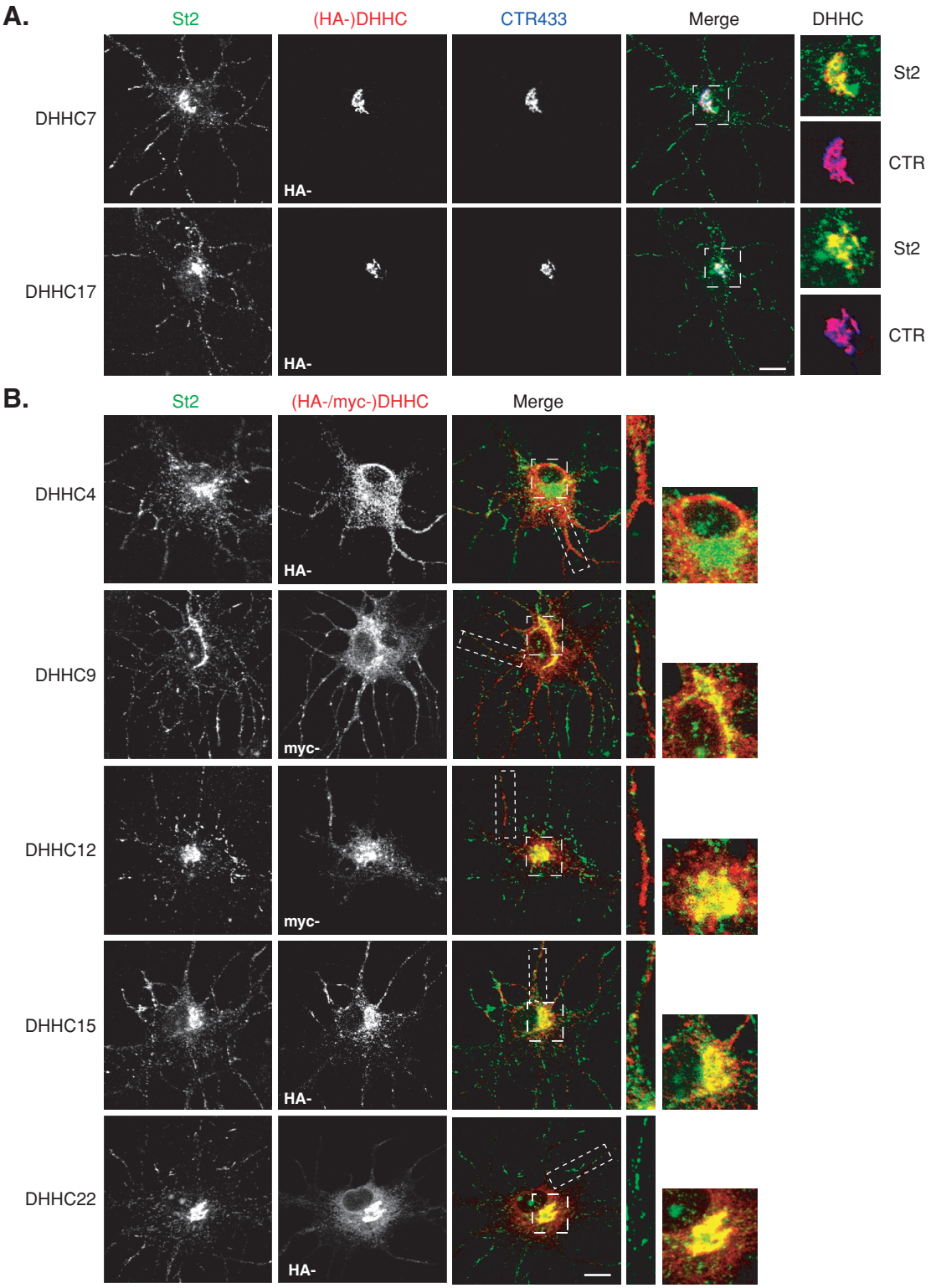

FIGURE 4: A specific set of DHHC PATs partially colocalized with stathmin 2 at the Golgi complex in hippocampal neurons. Hippocampal neurons transfected at 6 DIV with the indicated myc- or HA-tagged DHHCs were immunostained for endogenous stathmin 2 (St2, green), either HA or myc to visualize exogenous DHHCs (red), and CTR433 to visualize the Golgi complex (blue). (A) DHHC7 and -17 fully colocalized with CTR433 and displayed an extensive colocalization at the Golgi with endogenous stathmin 2 immunoreactivity, which was also present along neurites as a vesicle-like labeling. (B) As for DHHCs in (A), DHHC9, -12, and -15 colocalized with endogenous stathmin 2 at the Golgi (colocalization with CTR433 in Supplemental Figure S4), but were also present along neurites at vesicles not overlapping with those labeled for stathmin 2. DHHC22 colocalized with endogenous stathmin 2 at the Golgi but also showed an extra-Golgi labeling at the ER (colabeling with KDEL in Supplemental Figure S4). DHHC4 did not significantly colocalize with stathmin 2 but localized mainly to the ER (colabeling with KDEL in Supplemental Figure S4). Bars = 10 μM; boxed areas in the merged images are shown at higher magnification.

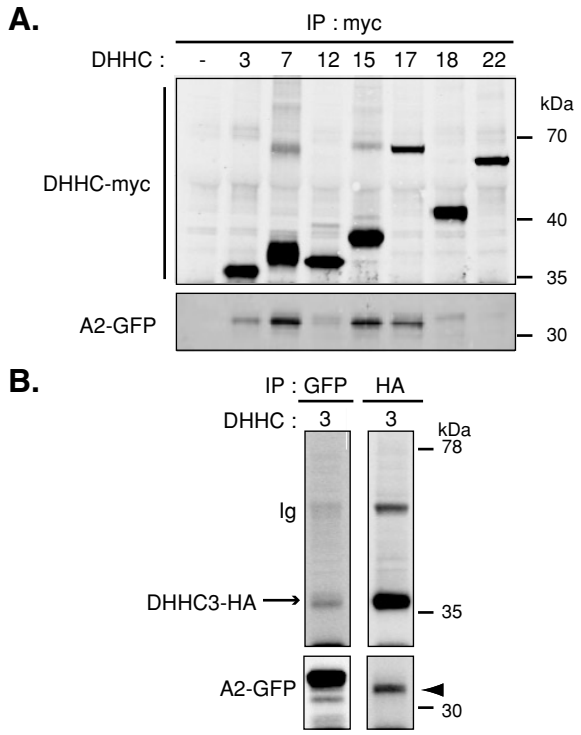

FIGURE 5: DHHC3, -7, -15, and -17 specifically interact with the targeting A domain of stathmin 2. The N-terminal targeting domain of stathmin 2 fused to GFP (A2-GFP) was cotransfected in HeLa cells with (A) either myc-tagged DHHC3, -7, -12, -15, -17, -18, or -22 or (B) HA-tagged DHHC3, and the corresponding cell lysates were tested for coimmunoprecipitation with A2-GFP using either anti-myc or anti-HA antibodies. (A) Immunoprecipitation of myc-tagged DHHCs revealed interaction of DHHC3, -7, -15, and -17 with A2-GFP. Cells with A2-GFP and the empty vector used for DHHC expression were processed as a control (lane 1). (B) Interaction between A2-GFP and DHHC3 was revealed after immunoprecipitation of both HA-tagged DHHC3 or A2-GFP. Anti-GFP antibody precipitated two major forms of A2-GFP, whereas anti-HA coimmunoprecipitated mainly the lower one (arrowhead). Note the presence of an IgG band corresponding to the immunoprecipitation of HA-DHHC3. These data are representative of three independent experiments that gave similar results.

-15, and -21. None of the other DHHC proteins were able to use stathmin 2 as a substrate. Furthermore, palmitoylation requires Cys-22 and/or Cys-24 because their double mutation to alanine blocked stathmin 2 palmitoylation. To compare whether the A2 domain and full-length stathmin 2 are palmitoylated by the same DHHCs, we also transfected each of the 23 DHHCs together with GFP-tagged A2 before the metabolic palmitoylation assay. These experiments showed that the same set of DHHCs (-2, -3, -7, -15, and -21) increased the incorporation of [^{3}H]palmitate into A2-GFP (Figure 6B). The same experimental procedure allowed us to compare the set of DHHC PATs that palmitoylate the various A domains of stathmin-related proteins (A2, A3, and A4). The level of palmitoylation of A2, A3, and A4 was estimated in comparison with [^{3}H]palmitate incorporation in full-length stathmin 2 as a reference. As presented in the comparative panel in Figure 6C, all A domains were preferentially palmitoylated by DHHC2, -3, -7, -15, and -21.

Altogether, consistent with their role in palmitoylation of stathmin-related proteins, specific Golgi resident PATs (DHHC3, -7, and -15) probably interact with the targeting domain of stathmins 2 and 3 to promote their Golgi-specific localization and trafficking. Note that DHHC2, which is only partially present at the Golgi, and DHHC21, which has been shown at the ER and at the plasma membrane (Ohno *et al.*, 2006), were also able to palmitoylate stathmins 2–4, probably revealing the possibility of non-Golgi palmitoylation.

Stathmin 2– and 3–specific PATs increase their stable membrane interaction

Because a key consequence of the palmitoylation of stathmins 2 and 3 is to promote membrane association, we predicted that specific DHHC overexpression might enhance the interaction of stathmins 2 and 3 with intracellular membranes. We examined the effects of Golgi-localized DHHC3, -7, -15, -22 and of DHHC21 on the membrane interaction of stathmins 2 and 3 when coexpressed within HeLa cells. Myc-tagged stathmin 1 and palmitoylation-defective mutant (C22A/C24A) stathmins 2 or 3 were used as nonpalmitoylated stathmin controls. Cotransfected cell extracts were subsequently fractionated into soluble (S) and membrane (M) fractions. As shown in Figure 7 and Supplemental Figure S6, all transfected DHHC PATs were detected in the membrane fraction, and overexpressed stathmin 1 was, as expected, exclusively in the soluble fraction, even in the presence of DHHC3. The majority, approximately 70%, of palmitoylation-deficient mutants of stathmin 2 or 3 (C22A/C24A) was also detected in the soluble fraction, with or without overexpressed DHHC3 (Figure 7, B and E; Supplemental Figure S6, A and C).

In the total HeLa extract (T), overexpressed stathmin 2 (as well as stathmin 3) migrated as several electrophoretic bands: an upper, double band (corresponding to various forms of stathmins) and a lower band, likely corresponding to a cleaved soluble form, as described in earlier studies (Stein *et al.*, 1988; Antonsson *et al.*, 1997; Lutjens *et al.*, 2000). When stathmins 2 and 3 were transfected alone, their upper forms were detected in both the soluble (45%) and membrane (55%) fractions, with a slightly higher level in the membrane one (Figure 7E and Supplemental Figure S6C), whereas the lower band was essentially in the soluble fraction. Cotransfection with DHHC3 promoted a significant increase in the membrane binding of stathmins 2 and 3 (70% and 80% of the total pool in the membrane fraction, respectively). This effect was specific, as an inactivating mutation within the putative catalytic domain (DHHC to DHHS: C/S) of DHHC3 abolished the ability of the enzyme to enhance membrane binding. Note that the inactive form of DHHC3 (C/S) was detected only by immunofluorescence on transfected cells (unpublished data).

Other specific DHHCs (-7, -15, and -21) also promoted a significant increase in the membrane association of stathmins 2 and 3 (Figure 7, D and F; Supplemental Figure S6, B and C). As a further test of DHHC specificity, we examined the effect on membrane association of stathmins 2 and 3 after coexpression with DHHC22, an enzyme that does not interact with or palmitoylate them (Figure 5 and 6 and Supplemental Figure S5); overexpression of this enzyme had no significant stimulatory effect on the membrane association of stathmins (Figure 7, D and F; Supplemental Figure S6, B and C). Note that all DHHC PATs tested are able to increase the expressed protein levels of transfected stathmins 2 and 3. This increase is specific because overexpression of DHHC3 did not induce any effect on the level of endogenous tubulin or stathmin 1 (Figure 7C).

These results clearly demonstrate that specific palmitoyl transferases are sufficient to drive stable membrane interaction of stathmin-related proteins in HeLa cells.

DISCUSSION

Proper subcellular localization of stathmins (Golgi/vesicles) is probably essential to promote their specific function, for example,

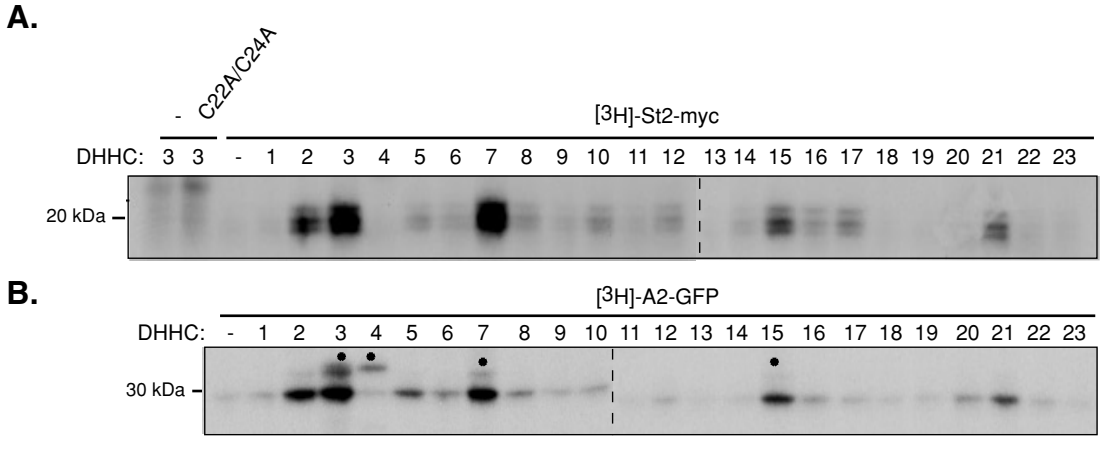

C.

	DHHC2	DHHC3	DHHC5	DHHC7	DHHC15	DHHC16	DHHC17	DHHC21
St2	++	+++	-	+++	+	-	+/-	+
A2	+++	+++	++	+++	+++	+/-	-	++
A3	++	+++	-	+++	++	-	-	++
A4	++	+++	-	+++	++	-	-	++

FIGURE 6: A specific set of DHHC PATs promotes stathmin 2–4 palmitoylation. Individual HA-tagged DHHCs were cotransfected in HEK293 cells with either (A) myc-tagged full-length (St2-myc) or (B) the GFP-tagged A2 targeting domain (A2-GFP) of stathmin 2. After metabolic labeling with [^{3}H]palmitic acid, proteins were separated by SDS–PAGE, and radioactive proteins were revealed by fluorography. Black dots indicate autopalmitoylation of expressed DHHC proteins. DHHC2, -3, -7, -15, and -21 enhanced the incorporation of [^{3}H]palmitic acid into (A) St2 or (B) A2. (A) No signal was present when the two sites of palmitoylation of stathmin 2 were mutated into alanine (C22A/C24A). (B) Note that DHHC5 was also able to use A2-GFP as a substrate. (C) In HEK293 cells cotransfected with individual HA-tagged DHHCs and one of the GFP-tagged targeting A domain of stathmins 2–4 (A2, A3, and A4-GFP), the level of palmitoylation of the latter was estimated in comparison with that of full-length stathmin 2 as a reference: +++ for stathmin 2 palmitoylation by DHHC3 and -7; ++ by DHHC2; + by DHHC15 and -21; +/– by DHHC17; and – by DHHC5 and -16.

by locally controlling microtubule dynamics during neuronal differentiation. We investigated here the molecular mechanisms that control this specific subcellular localization by identifying potential palmitoyl transferases responsible for this specific membrane attachment.

We identified three DHHC PATs (-3, -7, and -15) that can interact with, palmitoylate, and regulate membrane attachment of both stathmins 2 and 3. These PATs are exclusively or mostly localized at the Golgi in neurons, where we have shown that endogenous DHHC3 and stathmin 2 colocalize, as well as all three overexpressed PATs with endogenous stathmins 2 and 3. Indeed, palmitoylation of stathmins likely occurs at the Golgi because disruption of the Golgi structure by BFA (Lippincott-Schwartz *et al.*, 1989) prevents palmitoylation of stathmins 2 and 3. Nevertheless, it is unclear whether the BFA-induced inhibition of stathmins 2 and 3 palmitoylation is due to the loss of a functional Golgi apparatus or some indirect effect. Conversely, inhibition of stathmin 2 and 3 palmitoylation by 2-BP or BFA treatment disturbs the usual Golgi/vesicle localization of stathmins 2 and 3 with a major solubilization of these two proteins; loss of the Golgi localization as well as of the further vesicular trafficking were observed. Both treatments also showed small punctae differing from the usual vesicle labeling and depending on the drug treatments. Inhibiting palmitoylation of stathmins, however, does not redirect endogenous stathmins to mitochondria as previously observed for the only N-terminal A domain (Chauvin *et al.*, 2008), in agreement with the previously described potential inhibitory control of the SLD on the N-terminal targeting domain (Chauvin *et al.*, 2008). It is difficult to determine the nature of the small punctuate residual membrane compartments after 2-BP and BFA treatments because they both perturb vesicular trafficking from the Golgi complex. We can speculate that some unpalmitoylated stathmins may still be membrane bound. Indeed, their palmitoylation subdomain m possesses hydrophobic residues, whereas the Golgi specifying subdomain n includes charged residues (see Figure 1A), which might promote membrane binding, by hydrophobic/electrostatic interactions or by enhancing accessibility to PATs, before palmitoylation. This initial membrane interaction is shared with other neuronal proteins (Crouthamel *et al.*, 2008; Greaves *et al.*, 2009), such as the secretory vesicle associated protein CSP (Greaves and Chamberlain, 2006; Greaves *et al.*, 2008) and the γ-aminobutyric acid–synthesizing enzyme GAD-65 (Kanaani *et al.*, 2008). In this context, stathmins 2 and 3 might take advantage of a weak membrane affinity to bind transiently to cell membranes and "sample" them for DHHC PAT content. Upon association with Golgi membranes, they would then be recognized by the Golgi-specific PATs DHHC3, -7, and -15, which catalyze the palmitoylation and promote the stable anchoring of stathmin-related proteins, facilitating forward transport.

For many proteins, palmitoylation in the Golgi compartment does not seem to be involved in membrane anchoring but instead serves the function of mediating targeting to a particular post-Golgi compartment. For instance, palmitoylation of SNAP-25, GAP-43, and GAD-65 is not required for membrane binding but is essential

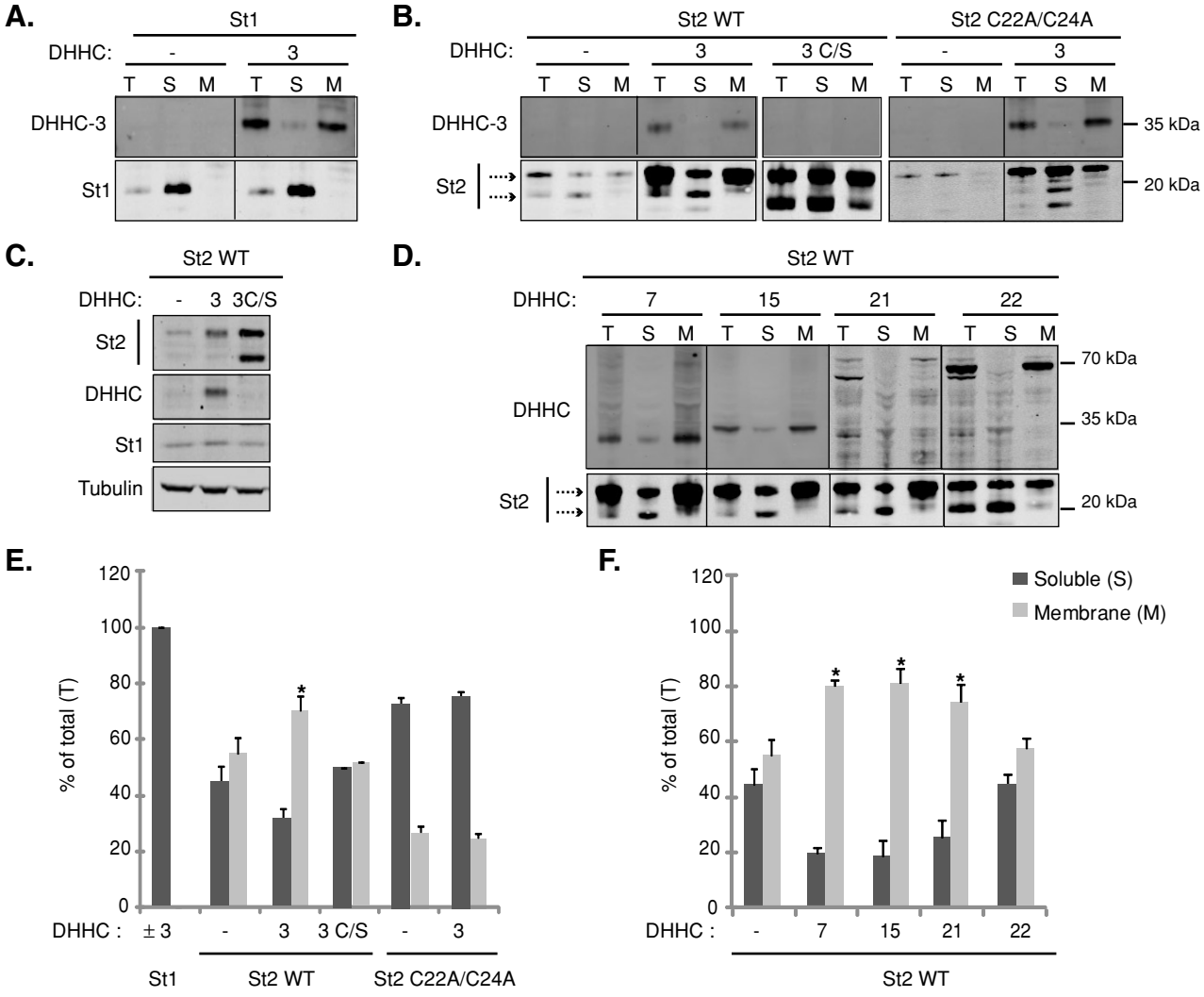

FIGURE 7: Stathmin 2 membrane binding is regulated by DHHC3, -7, -15, and -21. Individual HA-tagged DHHCs were cotransfected in HeLa cells with myc-tagged stathmin 1 (St1) or stathmin 2 (St2) (wild type or palmitoylation-deficient mutant C22A/C24A) and fractionated into soluble (S) and membrane (M) fractions. Aliquots of total cell extract (T) and equal volumes of the recovered S and M fractions were analyzed by Western blot using anti-myc for stathmins 1 and 2 and anti-HA (DHHC3, -7, -15, and -21) or anti-myc (DHHC22) antibodies for DHHCs. (A) While stathmin 1 was present exclusively in the soluble fraction after overexpressing, or not, DHHC3, exogenous DHHC3 by itself was only present in the membrane fraction. In the total extract (T), stathmin 2 migrated (arrows) as an upper double band and a lower cleaved one. (B) When stathmin 2 was transfected alone, the upper uncleaved forms were accumulated in both the soluble and membrane fractions, whereas its palmitoylation-deficient mutant C22A/C24A was enriched in the soluble fraction, in the presence, or not, of DHHC3. Inactive DHHC3 (C/S), which was not detected by Western blotting but was detected by immunofluorescence on transfected cells (unpublished data), had no effect on the distribution of stathmin 2, whereas (D) DHHC3, -7, -15, and -21 specifically and significantly enhanced its enrichment in the membrane fraction. Note that, despite a weak level of expression, DHHC21 was able to enhance stathmin 2 membrane binding. The "nonspecific" PAT DHHC22 was hardly efficient. Note that overexpression of all DHHCs induced an increase in the level of stathmin 2 expression, with (C) no change in the level of either endogenous stathmin 1 or tubulin, as shown for DHHC3. (E and F) Quantification of the membrane and the soluble pools of stathmin 2 transfected together with each of the DHHC proteins. The intensity of the upper forms of stathmin 2 in each fraction was quantified in comparison with their intensity in the total extract (T). Values are mean ± SEM (n = 3). The statistical significance of differences between the percentage of stathmin 2 in membrane fractions, when coexpressed with DHHCs or not, was assessed by a Student's *t* test. *p < 0.05.

for their sorting at the *trans*-Golgi network (TGN) into vesicles that are delivered to their appropriate subcellular localization in the axon (Bijlmakers and Marsh, 2003; Kanaani *et al.*, 2008). We can speculate that the large pool of stathmins 2–4 is palmitoylated and stored at the Golgi complex and, upon specific signals, palmitoylated stathmins 2–4 are released through vesicular pathways and targeted to specific areas where their microtubule-regulating activities is needed. Stathmins 2–4 probably shuttle to specific membranes present within the growth cones and along neurites, especially at branch sites (Mori and Morii, 2002; Grenningloh *et al.*, 2004; Tararuk *et al.*, 2006; Poulain and Sobel, 2007; Poulain *et al.*, 2008). At these sites, their microtubule-regulating activity might then be controlled by phosphorylation/dephosphorylation (Tararuk *et al.*, 2006; Poulain and Sobel, 2007, 2010). Regulation of protein

shuttling by palmitoylation/depalmitoylation would provide an additional regulatory mechanism for the functions of stathmins in neurons during their differentiation. We were not able so far to reveal a change in local microtubule dynamics at the neuronal growth cone, or changes in neuronal morphogenesis by overexpressing PATs, either because of technical challenges or likely because of the complex regulatory networks and compensatory mechanisms involved. In addition, regulation of stathmin membrane anchoring by depalmitoylation might add another layer of regulation of stathmin activities. To understand the whole process of these regulations, it will be necessary to characterize the involvement and roles of potential depalmitoylating enzymes.

In mammalian genomes, 23 DHHC genes and proteins are predicted (Fukata and Fukata, 2010) and classified according to their phylogeny into several subfamilies; for example, regarding the DHHC PATs that were able to palmitoylate stathmins, DHHC3 and -7 belong to the same subfamily and possess a broad substrate specificity (Hayashi *et al.*, 2005; Ponimaskin *et al.*, 2008; Tsutsumi *et al.*, 2008), whereas DHHC2 and -15 are part of another subfamily and are more specific for PSD-95 and GAP-43 (Fukata *et al.*, 2004). DHHC21 is found far from these two subfamilies, and preferably palmitoylates eNOS, Lck, Fyn, and $G\alpha_{i2}$ (Fukata and Fukata, 2010). Therefore stathmins 2 and 3 can be added to the list of DHHC3 and -7 substrates but also and interestingly to the restricted group of DHHC21 known substrates. Our attempts to deplete DHHC3 proteins by siRNA in neurons were unsuccessful in mislocalizing stathmin 2 or 3 (unpublished data), suggesting that other DHHC candidates might be able to compensate for the absence of this DHHC PAT.

The substrate variability of these DHHC PATs suggests that specific protein palmitoylation is orchestrated by diverse stimuli. Regulation of DHHC PAT activity by posttranslational modification or action of second messengers, such as cAMP or metal ions, or regulation of DHHC distribution by extracellular stimulation might play a crucial role (Tsutsumi *et al.*, 2008). Extracellular signals translocate specific DHHC PATs and create a new route for substrate shuttling between palmitoylation and depalmitoylation loci, leading to efficient and precise substrate targeting. Such a compartmentalized regulatory mechanism may contribute to spatiotemporal regulation of signaling molecules in polarized neurons (Noritake *et al.*, 2009). In this context, we can speculate that neuronal activity, which has been shown to change the phosphorylation status of stathmin 2 (Morii *et al.*, 2006), or growth factors such as nerve growth factor (NGF) or brain-derived neuronal factor (BDNF) that up-regulate the expression of stathmin 2 (Stein *et al.*, 1988; Imamura *et al.*, 2006), may control the activity of individual DHHC PATs and then regulate subcellular localization and local function of stathmins.

Our results provide new evidence for the central role of stathmin palmitoylation in their specific subcellular localization and trafficking. Now, we know that the Golgi resident DHHC3, -7, and -15 are able to interact with and palmitoylate stathmin-related proteins, to regulate their membrane attachment. This interaction might also promote stabilization of stathmins, by an unknown mechanism however independent of palmitoylation itself, because the inactive form of DHHC3, or DHHC22, which did not palmitoylate stathmins, was as efficient. By regulating palmitoylation of stathmins, extracellular stimuli control their local functions by preventing or promoting their appropriate specific membrane localization within neurons. Further studies will be required to identify the extracellular stimuli that control the activities of these DHHC PATs and therefore palmitoylation of stathmins in the context of their biological activities and regulation.

MATERIALS AND METHODS

Reagents, plasmids, and antibodies

BFA and 2-BP were obtained from Sigma-Aldrich (St. Louis, MO). DMEM-Glutamax, MEM, Glutamine, fetal bovine and horse serum, Lipofectamine 2000, penicillin/streptomycin, B27, Neurobasal medium, NuPAGE LSD sample buffer, 12% NuPAGE bisTris gels, and OptiMEM were obtained from Invitrogen Life Technologies (Carlsbad, CA).

Myc-tagged DHHCs were generous gifts of A. Kihara (Hokkaido University, Sapporo, Japan). Palmitoylation-deficient stathmin mutants have been previously described (Chauvin *et al.*, 2008), and cDNAs encoding DHHC proteins were cloned in PEF-Bos-HA (BD Biosciences, San Jose, CA) as previously described (Fukata *et al.*, 2004).

Commercial antibodies and their dilutions (vol/vol) (IF: immunofluorescence; IP: immunoprecipitation; WB: Western blot) were: mouse monoclonal anti-KDEL, a marker of the ER (IF 1:200) (StressGen, Ann Arbor, MI), anti–α tubulin (WB 1:10,000) (Sigma), polyclonal anti-myc (IF 1:500) (Cell Signaling Technology, Danvers, MA), mouse monoclonal anti-GFP, anti-myc, and rat monoclonal anti-HA (IF 1:500; WB 1:1000; IP 0.2 μg/100 μl) (Roche Diagnostics, Basel Switzerland), polyclonal anti-DHHC3 (IF 1:300) (Abcam, Cambridge, UK), monoclonal anti–stathmin 2 (IF 1:500) (clone L5/1; NeuroMab, UC Davis, CA), Alexa 488–, Alexa 546–, and Alexa 633–conjugated secondary antibodies (IF 1:1000) (Invitrogen Life Technologies), and IRDye 800- or 700-conjugated secondary antibodies (WB 1:5000) (Rockland Immunochemicals, Gilbertsville, PA).

Rabbit polyclonal sera directed against stathmin 1 (WB 1:10,000), stathmin 2, and stathmin 3 (WB 1:2000) have been described previously (Gavet *et al.*, 2002), and polyclonal antibodies raised against stathmin 2 or stathmin 3 (IF 1:400) were purified on their antigens (Poulain and Sobel, 2007). Mouse monoclonal antibody to DHHC2 has been previously described (Noritake *et al.*, 2009). Monoclonal antibody CTR433, a marker of the median Golgi (IF 1:10) was a generous gift of M. Bornens (Institut Curie, Paris, France).

Cell culture

Cortical and hippocampal neurons were isolated from rat embryos (E18) (Charles River, L'Arbresle, France) and cultured in B27-supplemented neurobasal medium as previously described (Charbaut *et al.*, 2005). Cells were plated on poly-ornithine–coated coverslips at 5×10^5 cells/9.6 cm^2 dish for Western blots and ABE assays, and 7.6×10^4 cells/3.5 cm^2 dish for drug treatments and neuron transfection.

HeLa and HEK293 cells were obtained from American Type Culture Collection (ATCC; Manassas, VA) and maintained in DMEM-Glutamax supplemented with 10% decomplemented fetal bovine serum and 1% penicillin/streptomycin at 37°C in a humidified atmosphere containing 5% CO_2.

ABE assay

The ABE method was performed as described (Noritake *et al.*, 2009) with slight modifications. Cortical neurons (6 DIV), treated or not with different drugs, were washed twice with phosphate-buffered saline (PBS) containing 20 mM NEM and solubilized with 0.1 ml of lysis buffer (LB: 50 mM Tris-HCl, pH 7.5, 5 mM EDTA, and 50 mM NaCl) containing 2% SDS and 20 mM NEM. After 15 min of extraction, LB with 2% Triton X-100 and 20 mM NEM was added to a final volume of 1 ml and incubated for 1 h at 4°C. After centrifugation at 20,000 × *g* for 10 min, the supernatants were precipitated by chloroform–methanol (CM) (Wessel and Flugge, 1984). Precipitated

protein was solubilized in 0.2 ml of buffer SB (50 mM Tris-HCl, pH 7.5, 5 mM EDTA, and 4% SDS) containing 20 mM NEM at 37°C for 10 min. The protein was diluted in 0.8 ml of LB with 0.2% Triton X-100 and 1 mM NEM, and incubated overnight at 4°C. NEM was removed by three sequential CM precipitations. Precipitated protein was solubilized in 0.2 ml of buffer SB, and then 0.8 ml of HB (1 M HAM, pH 7.5, 150 mM NaCl, 0.2% Triton X-100, and 1 mM biotin-HPDP) or buffer TB (1 M Tris-HCl, pH 7.5, 150 mM NaCl, 0.2% Triton X-100, and 1 mM biotin-HPDP was added. The mixture was incubated for 1 h at room temperature. Free HAM and biotin-HPDP were removed by CM precipitations. The precipitated protein was solubilized in 0.1 ml of buffer UB (50 mM Tris-HCl, pH 7.5, 5 mM EDTA, and 2% SDS) and diluted in 0.9 ml of LB containing 0.2% Triton X-100. After brief centrifugation, the supernatant was incubated with 30 µl of NeutrAvidin-agarose (Thermo Fisher Scientific) for 1 h at 4°C. After the beads were washed with LB containing 0.1% SDS and 0.2% Triton X-100, bound proteins were suspended in NuPAGE LSD sample buffer with 10 mM dithiothreitol (DTT). The samples were subjected to SDS–PAGE and Western blotting with indicated antibodies.

Transfection

Neurons were transfected at 6 DIV using Lipofectamine 2000. For 18-mm coverslips, 1 µg of DNA was diluted in 50 µl of OptiMEM, and 0.5 µl of Lipofectamine 2000 was added to 50 µl of OptiMEM. After a 5-min incubation, these two solutions were mixed and incubated for 20 min at room temperature. Then this mixture was added directly to the culture medium. HeLa and HEK293 cells were seeded at 12,500 cells/cm^2 in 35-mm dishes and transfected 24 h after seeding using Lipofectamine 2000 (250 µl of OptiMEM, 3 µl of Lipofectamine 2000, and 1 µg of plasmid DNA).

Metabolic labeling

Screening of the candidate PATs was performed in HEK293T cells as described previously (Fukata *et al.*, 2004, 2006). To detect palmitoylation of transfected stathmins 2–4, cells were metabolically labeled with 0.5 mCi/ml [^{3}H]palmitate-containing medium for 4 h, 24 h after transfection. After labeling, cells were washed once with ice-cold PBS and lysed in SDS–PAGE sample buffer (62.5 mM Tris-HCl, pH 6.8, 10% glycerol, 2% SDS and 0.001% bromophenol blue) with 10 mM DTT. Proteins were resolved by SDS–PAGE. After fixing the gels for 30 min in a fixing solution (isopropanol/water/acetic acid; 25:65:10), the gel was treated with Amplify fluorographic reagent (GE Healthcare) for 30 minutes, dried under vacuum, and exposed to x-ray film (Kodak BioMax MS) without screen at –80°C for 24 h.

Immunoprecipitation and Western blot

For immunoprecipitation, transfected HeLa cells were lysed in 200 µl of ice-cold immunoprecipitation buffer containing 50 mM Tris-HCl, pH 7.4, 10% glycerol, 125 mM NaCl, 1% Triton X-100, 5.3 mM NaF, 1.5 mM NaP, 1 mM orthovanadate, 1 mg/ml protease inhibitor cocktail (Complete; Roche). Cells were agitated at 4°C for 20 min before the insoluble material was removed by centrifugation at 20,000 × *g* for 15 min. Samples were then incubated with anti-myc or anti-HA (for DHHC constructs) or anti-GFP (for GFP-tagged A forms constructs) for 2 h at 4°C under rotation. G protein–coupled sepharose beads (Roche Diagnostics, Mannheim, Germany) were then added to the protein extracts and incubated at 4°C overnight. Beads were washed three times with immunoprecipitation buffer. Proteins in both cell lysates and immunoprecipitates were diluted and denatured in NuPAGE LSD sample buffer, separated on 12% NuPAGE bisTris gels, and then transferred to 0.45-µm nitrocellulose membranes (Whatman Schleicher & Schuell, Dassel, Germany) in 25 mM Tris-HCl, 192 mM glycine, 20% ethanol. Membranes were blocked with 5% milk in 12 mM Tris-HCl, pH 7.4, 160 mM NaCl, 0,1% Triton X-100 (Buffer A) and then incubated for 1 h at room temperature or overnight at 4°C with the corresponding primary antibody. After three washes in buffer A, the membranes were incubated for 1 h at room temperature with IRDye-coupled secondary antibodies (Rockland Immunochemicals) against rabbit or mouse immunoglobulins (IgGs), which were detected with an Odyssey Imaging System (LI-COR Biosciences, Lincoln, NE) providing a linear response in a broad range of infrared fluorescence intensities. Signals were quantified with LI-COR software.

Cell fractionation

HeLa cells (24 h after transfection) and hippocampal neurons were homogenized in a Dounce homogenizer in 10 mM HEPES, 250 mM sucrose, 1 mM EDTA, pH 7.4, with an anti-protease cocktail (Complete; Roche) at 4°C and fractionated by differential centrifugation. The homogenate was first centrifuged at 850 × *g* for 5 min at 4°C to obtain a postnuclear supernatant. Then this supernatant was centrifuged at 10,000 × *g* for 10 min at 4°C to remove mitochondria. The resulting supernatant was finally centrifuged at 400,000 × *g* for 6 min at 4°C to obtain the soluble (supernatant) and membrane (pellet) fractions. Equal volumes of these fractions were analyzed by SDS–PAGE. Quantification of the membrane and the soluble pools of stathmins 2 and 3 were analyzed and compared to the total extract (T) and expressed as a percentage of the total.

Immunofluorescence

Nontransfected or transfected neurons (17 h after transfection) were fixed at 37°C with 2% (wt/vol) paraformaldehyde (PFA) for 5 min and then with 4% PFA for 10 min. For staining of DHHC2, neurons were fixed with methanol for 10 min at –30°C. After five washes with PBS, neurons were permeabilized with 0.1% Triton X-100 in PBS for 6 min and blocked for 1 h with 3% bovine serum albumin in PBS. Neurons were then incubated for 1 h at room temperature with appropriate primary antibodies in blocking buffer. After five washes with 0.1% Tween 20 in PBS, neurons were incubated for 1 h with Alexa 488– and/or 546– and/or 633–coupled secondary antibody against rabbit, mouse, or rat IgG. After five washes with 0.1% Tween 20 in PBS, neurons were washed once in water before mounting in a Mowiol solution.

Confocal fluorescence microscopy was performed at the Institut du Fer à Moulin Cell Imaging Facility with an SP2 confocal microscope (Leica Microsystems, Wetzlar, Germany). Confocal images in Figures 2–4 and Supplemental Figures S2–4 are single confocal sections from high-resolution stacks, representative in each case of three independent experiments.

Statistical analysis

In Figures 2 and 7, and in Supplemental Figure S2, results are expressed as means ± SEM (n = 3 independent experiments). In Figure 2 and Supplemental Figure S2, the statistical significance of differences between the percentage of endogenous stathmins 2 and 3 in membrane fractions of treated conditions (2-BP or BFA) compared to the one in the absence of treatment was assessed by a Student's *t* test: *$p < 0.05$, **$p < 0.01$. In Figure 7, the statistical significance of differences between the percentage of stathmin 2 in membrane fractions of each DHHC's coexpression compared with stathmin 2 in the absence of exogenous DHHC PAT was assessed by a Student's *t* test: *$p < 0.05$.

ACKNOWLEDGMENTS

We thank F. Poulain, C. Plestant, C. Boscher, and A. Maucuer for discussions throughout this work. We are grateful to A. Andrieux and T. Galli for insightful discussions. We also thank M. Bornens for the generous gifts of CTR433 antibodies and Y. Ohno and A. Kihara for providing myc-tagged DHHC constructs. Fluorescence and confocal microscopy was performed at the Institut du Fer à Moulin Imaging facility. This work was supported by the Institut National de la Santé et de la Recherche Médicale (INSERM), the Université Pierre et Marie Curie (UPMC), The Agence Nationale de la Recherche (ANR grant Neudifstat), and the Association pour la Recherche contre le Cancer (ARC). A.L. is supported by the Ministère de l'Enseignement Supérieur et de la Recherche (MESR).

REFERENCES

Antonsson B, Montessuit S, Di Paolo G, Lutjens R, Grenningloh G (1997). Expression, purification, and characterization of a highly soluble N-terminal-truncated form of the neuron-specific membrane-associated phosphoprotein SCG10. Protein Expr Purif 9, 295–300.

Bartels DJ, Mitchell DA, Dong X, Deschenes RJ (1999). Erf2, a novel gene product that affects the localization and palmitoylation of Ras2 in Saccharomyces cerevisiae. Mol Cell Biol 19, 6775–6787.

Belmont L, Mitchison T, Deacon HW (1996). Catastrophic revelations about Op18/stathmin. Trends Biochem Sci 21, 197–198.

Bijlmakers MJ, Marsh M (2003). The on-off story of protein palmitoylation. Trends Cell Biol 13, 32–42.

Charbaut E, Chauvin S, Enslen H, Zamaroczy S, Sobel A (2005). Two separate motifs cooperate to target stathmin-related proteins to the Golgi complex. J Cell Sci 118, 2313–2323.

Charbaut E, Curmi PA, Ozon S, Lachkar S, Redeker V, Sobel A (2001). Stathmin family proteins display specific molecular and tubulin binding properties. J Biol Chem 276, 16146–16154.

Chauvin S, Poulain FE, Ozon S, Sobel A (2008). Palmitoylation of stathmin family proteins domain A controls Golgi versus mitochondrial subcellular targeting. Biol Cell 100, 577–589.

Chisari M, Saini DK, Kalyanaraman V, Gautam N (2007). Shuttling of G protein subunits between the plasma membrane and intracellular membranes. J Biol Chem 282, 24092–24098.

Crouthamel M, Thiyagarajan MM, Evanko DS, Wedegaertner PB (2008). N-terminal polybasic motifs are required for plasma membrane localization of Galpha(s) and Galpha(q). Cell Signal 20, 1900–1910.

Curmi PA, Andersen SS, Lachkar S, Gavet O, Karsenti E, Knossow M, Sobel A (1997). The stathmin/tubulin interaction in vitro. J Biol Chem 272, 25029–25036.

Curmi PA, Gavet O, Charbaut E, Ozon S, Lachkar-Colmerauer S, Manceau V, Siavoshian S, Maucuer A, Sobel A (1999). Stathmin and its phosphoprotein family: general properties, biochemical and functional interaction with tubulin. Cell Struct Funct 24, 345–357.

Di Paolo G, Lutjens R, Pellier V, Stimpson SA, Beuchat MH, Catsicas S, Grenningloh G (1997). Targeting of SCG10 to the area of the Golgi complex is mediated by its NH2-terminal region. J Biol Chem 272, 5175–5182.

el-Husseini Ael D, Bredt DS (2002). Protein palmitoylation: a regulator of neuronal development and function. Nat Rev Neurosci 3, 791–802.

El-Husseini Ael D, Schnell E, Dakoji S, Sweeney N, Zhou Q, Prange O, Gauthier-Campbell C, Aguilera-Moreno A, Nicoll RA, Bredt DS (2002). Synaptic strength regulated by palmitate cycling on PSD-95. Cell 108, 849–863.

Fujiwara T, Oda K, Yokota S, Takatsuki A, Ikehara Y (1988). Brefeldin A causes disassembly of the Golgi complex and accumulation of secretory proteins in the endoplasmic reticulum. J Biol Chem 263, 18545–18552.

Fukata M, Fukata Y, Adesnik H, Nicoll RA, Bredt DS (2004). Identification of PSD-95 palmitoylating enzymes. Neuron 44, 987–996.

Fukata Y, Fukata M (2010). Protein palmitoylation in neuronal development and synaptic plasticity. Nat Rev Neurosci 11, 161–175.

Fukata Y, Iwanaga T, Fukata M (2006). Systematic screening for palmitoyl transferase activity of the DHHC protein family in mammalian cells. Methods 40, 177–182.

Gavet O, El Messari S, Ozon S, Sobel A (2002). Regulation and subcellular localization of the microtubule-destabilizing stathmin family phosphoproteins in cortical neurons. J Neurosci Res 68, 535–550.

Gavet O, Ozon S, Manceau V, Lawler S, Curmi P, Sobel A (1998). The stathmin phosphoprotein family: intracellular localization and effects on the microtubule network. J Cell Sci 111, Pt 22, 3333–3346.

Gigant B, Curmi PA, Martin-Barbey C, Charbaut E, Lachkar S, Lebeau L, Siavoshian S, Sobel A, Knossow M (2000). The 4 A X-ray structure of a tubulin:stathmin-like domain complex. Cell 102, 809–816.

Gigant B, Wang C, Ravelli RB, Roussi F, Steinmetz MO, Curmi PA, Sobel A, Knossow M (2005). Structural basis for the regulation of tubulin by vinblastine. Nature 435, 519–522.

Greaves J, Chamberlain LH (2006). Dual role of the cysteine-string domain in membrane binding and palmitoylation-dependent sorting of the molecular chaperone cysteine-string protein. Mol Biol Cell 17, 4748–4759.

Greaves J, Prescott GR, Fukata Y, Fukata M, Salaun C, Chamberlain LH (2009). The hydrophobic cysteine-rich domain of SNAP25 couples with downstream residues to mediate membrane interactions and recognition by DHHC palmitoyl transferases. Mol Biol Cell 20, 1845–1854.

Greaves J, Salaun C, Fukata Y, Fukata M, Chamberlain LH (2008). Palmitoylation and membrane interactions of the neuroprotective chaperone cysteine-string protein. J Biol Chem 283, 25014–25026.

Grenningloh G, Soehrman S, Bondallaz P, Ruchti E, Cadas H (2004). Role of the microtubule destabilizing proteins SCG10 and stathmin in neuronal growth. J Neurobiol 58, 60–69.

Hayashi T, Rumbaugh G, Huganir RL (2005). Differential regulation of AMPA receptor subunit trafficking by palmitoylation of two distinct sites. Neuron 47, 709–723.

Huang K, El-Husseini A (2005). Modulation of neuronal protein trafficking and function by palmitoylation. Curr Opin Neurobiol 15, 527–535.

Huang K, Sanders S, Singaraja R, Orban P, Cijsouw T, Arstikaitis P, Yanai A, Hayden MR, El-Husseini A (2009). Neuronal palmitoyl acyl transferases exhibit distinct substrate specificity. FASEB J 23, 2605–2615.

Imamura K, Morii H, Nakadate K, Yamada T, Mataga N, Watanabe Y, Mori N (2006). Brain-derived neurotrophic factor enhances expression of superior cervical ganglia clone 10 in lateral geniculate nucleus and visual cortex of developing kittens. Eur J Neurosci 23, 637–648.

Iwanaga T, Tsutsumi R, Noritake J, Fukata Y, Fukata M (2009). Dynamic protein palmitoylation in cellular signaling. Prog Lipid Res 48, 117–127.

Jourdain L, Curmi P, Sobel A, Pantaloni D, Carlier MF (1997). Stathmin: a tubulin-sequestering protein which forms a ternary T2S complex with two tubulin molecules. Biochemistry 36, 10817–10821.

Kanaani J, Patterson G, Schaufele F, Lippincott-Schwartz J, Baekkeskov S (2008). A palmitoylation cycle dynamically regulates partitioning of the GABA-synthesizing enzyme GAD65 between ER-Golgi and post-Golgi membranes. J Cell Sci 121, 437–449.

Kang R *et al.* (2008). Neural palmitoyl-proteomics reveals dynamic synaptic palmitoylation. Nature 456, 904–909.

Keller CA, Yuan X, Panzanelli P, Martin ML, Alldred M, Sassoe-Pognetto M, Luscher B (2004). The gamma2 subunit of GABA(A) receptors is a substrate for palmitoylation by GODZ. J Neurosci 24, 5881–5891.

Klausner RD, Donaldson JG, Lippincott-Schwartz J (1992). Brefeldin A: insights into the control of membrane traffic and organelle structure. J Cell Biol 116, 1071–1080.

Lachkar S, Lebois M, Steinmetz MO, Guichet A, Lal N, Curmi PA, Sobel A, Ozon S (2010). Drosophila stathmins bind tubulin heterodimers with high and variable stoichiometries. J Biol Chem 285, 11667–11680.

Linder ME, Deschenes RJ (2004). Model organisms lead the way to protein palmitoyltransferases. J Cell Sci 117, 521–526.

Linder ME, Deschenes RJ (2007). Palmitoylation: policing protein stability and traffic. Nat Rev Mol Cell Biol 8, 74–84.

Lippincott-Schwartz J, Yuan LC, Bonifacino JS, Klausner RD (1989). Rapid redistribution of Golgi proteins into the ER in cells treated with brefeldin A: evidence for membrane cycling from Golgi to ER. Cell 56, 801–813.

Lobo S, Greentree WK, Linder ME, Deschenes RJ (2002). Identification of a Ras palmitoyltransferase in Saccharomyces cerevisiae. J Biol Chem 277, 41268–41273.

Lutjens R, Igarashi M, Pellier V, Blasey H, Di Paolo G, Ruchti E, Pfulg C, Staple JK, Catsicas S, Grenningloh G (2000). Localization and targeting of SCG10 to the trans-Golgi apparatus and growth cone vesicles. Eur J Neurosci 12, 2224–2234.

Mori N, Morii H (2002). SCG10-related neuronal growth-associated proteins in neural development, plasticity, degeneration, and aging. J Neurosci Res 70, 264–273.

Morii H, Yamada T, Nakano I, Coulson JM, Mori N (2006). Site-specific phosphorylation of SCG10 in neuronal plasticity: role of Ser73 phosphorylation by N-methyl D-aspartic acid receptor activation in rat hippocampus. Neurosci Lett 396, 241–246.

Noritake J *et al.* (2009). Mobile DHHC palmitoylating enzyme mediates activity-sensitive synaptic targeting of PSD-95. J Cell Biol 186, 147–160.

Ohno Y, Kihara A, Sano T, Igarashi Y (2006). Intracellular localization and tissue-specific distribution of human and yeast DHHC cysteine-rich domain-containing proteins. Biochim Biophys Acta 1761, 474–483.
Ozon S, Byk T, Sobel A (1998). SCLIP: a novel SCG10-like protein of the stathmin family expressed in the nervous system. J Neurochem 70, 2386–2396.
Ozon S, Maucuer A, Sobel A (1997). The stathmin family—molecular and biological characterization of novel mammalian proteins expressed in the nervous system. Eur J Biochem 248, 794–806.
Ponimaskin E *et al.* (2008). Fibroblast growth factor-regulated palmitoylation of the neural cell adhesion molecule determines neuronal morphogenesis. J Neurosci 28, 8897–8907.
Poulain FE, Chauvin S, Wehrle R, Desclaux M, Mallet J, Vodjdani G, Dusart I, Sobel A (2008). SCLIP is crucial for the formation and development of the Purkinje cell dendritic arbor. J Neurosci 28, 7387–7398.
Poulain FE, Sobel A (2007). The "SCG10-LIke Protein" SCLIP is a novel regulator of axonal branching in hippocampal neurons, unlike SCG10. Mol Cell Neurosci 34, 137–146.
Poulain FE, Sobel A (2010). The microtubule network and neuronal morphogenesis: Dynamic and coordinated orchestration through multiple players. Mol Cell Neurosci 43, 15–32.
Ravelli RB, Gigant B, Curmi PA, Jourdain I, Lachkar S, Sobel A, Knossow M (2004). Insight into tubulin regulation from a complex with colchicine and a stathmin-like domain. Nature 428, 198–202.
Resh MD (2006). Palmitoylation of ligands, receptors, and intracellular signaling molecules. Sci STKE 2006, re14.
Rocks O, Peyker A, Bastiaens PI (2006). Spatio-temporal segregation of Ras signals: one ship, three anchors, many harbors. Curr Opin Cell Biol 18, 351–357.
Roth AF, Feng Y, Chen L, Davis NG (2002). The yeast DHHC cysteine-rich domain protein Akr1p is a palmitoyl transferase. J Cell Biol 159, 23–28.
Roth AF, Wan J, Bailey AO, Sun B, Kuchar JA, Green WN, Phinney BS, Yates JR, 3rd, Davis NG (2006). Global analysis of protein palmitoylation in yeast. Cell 125, 1003–1013.
Smotrys JE, Linder ME (2004). Palmitoylation of intracellular signaling proteins: regulation and function. Annu Rev Biochem 73, 559–587.
Sobel A (1991). Stathmin: a relay phosphoprotein for multiple signal transduction?. Trends Biochem Sci 16, 301–305.
Stein R, Mori N, Matthews K, Lo LC, Anderson DJ (1988). The NGF-inducible SCG10 mRNA encodes a novel membrane-bound protein present in growth cones and abundant in developing neurons. Neuron 1, 463–476.
Tararuk T *et al.* (2006). JNK1 phosphorylation of SCG10 determines microtubule dynamics and axodendritic length. J Cell Biol 173, 265–277.
Togano T, Kurachi M, Watanabe M, Grenningloh G, Igarashi M (2005). Role of Ser50 phosphorylation in SCG10 regulation of microtubule depolymerization. J Neurosci Res 80, 475–480.
Tsutsumi R, Fukata Y, Fukata M (2008). Discovery of protein-palmitoylating enzymes. Pflugers Arch 456, 1199–1206.
Tsutsumi R, Fukata Y, Noritake J, Iwanaga T, Perez F, Fukata M (2009). Identification of G protein alpha subunit-palmitoylating enzyme. Mol Cell Biol 29, 435–447.
Wedegaertner PB, Bourne HR (1994). Activation and depalmitoylation of Gs alpha. Cell 77, 1063–1070.
Wessel D, Flugge UI (1984). A method for the quantitative recovery of protein in dilute solution in the presence of detergents and lipids. Anal Biochem 138, 141–143.